ONCOIMMUNOLOGY
2023, VOL. 12, NO. 1, 2246322
https://doi.org/10.1080/2162402X.2023.2246322

Taylor & Francis
Taylor & Francis Group

ORIGINAL RESEARCH

OPEN ACCESS Check for updates

TNBC-derived Gal3BP/Gal3 complex induces immunosuppression through CD45 receptor

Annat Raiter[a], Julia Lipovetsky[b], Asaf Stenbac[a], Ido Lubin[a], and Rinat Yerushalmi[a,b]

[a]Felsenstein Medical Research Center, Tel Aviv University, Faculty of Medicine, Petach Tikva, Israel; [b]Institute of Oncology, Davidoff Cancer Center, Rabin Medical Center, Petach Tikva, Israel

ABSTRACT

A preliminary study investigating immunotherapy strategies for aggressive triple negative breast cancer (TNBC) revealed an overexpression of genes involved in the release of extracellular vesicles (EVs). Proteins expressed by EVs play a role in reprogramming the tumor microenvironment and impeding effective responses to immunotherapy. Galectin 3 (Gal3), found in the extracellular space of breast cancer cells, downregulates T-cell receptor expression. Gal3 binds to several receptors, including CD45, which is required for T-cell receptor activation. Previously, we reported a novel tumor escape mechanism, whereby TNBC cells suppress immune cells through CD45 intracellular signals. The objective of this study was to determine the potential association of Gal3 with TNBC-secreted EVs induction of immunosuppression via the CD45 signaling pathway. EVs were isolated from MDA-MB-231 cells and the plasma of patients with TNBC. Mass spectrometry revealed the presence of Gal3 binding protein (Gal3BP) in the isolated small EVs, which interacted with TNBC secreted Gal3. Gal3BP and Gal3 form a complex that induces a significant increase in T-regulatory cells in peripheral blood mononuclear cells (PBMCs). This increase correlates with a significant increase in suppressive interleukins 10 and 35. Blocking the CD45 receptor in PBMCs cultured with tumor-derived EVs impeded the immunosuppression exerted by the Gal3BP/Gal3 complex. This led to an increase in IFN-γ and the activation of CD4, CD8 and CD56 effector cells. This study suggests a tumor escape mechanism that may contribute to the development of a different immunotherapy strategy that complements current therapies used for TNBC.

ARTICLE HISTORY
Received 16 May 2023
Revised 7 August 2023
Accepted 7 August 2023

KEYWORDS
Galectin 3; Galectin 3 binding protein; immunosuppression; small extracellular vesicles; TNBC

Introduction

Triple negative breast cancer (TNBC) is an aggressive tumor which predominantly affects young women. TNBC is often diagnosed at a more advanced stage and lacks targeted therapies.[1,2] Currently, treatment strategies are comprised of conventional chemotherapy (taxanes, anthracycline and platinum), immunotherapy and surgery. Multiple reports suggest the use of immunotherapeutic strategies for aggressive metastatic TNBC, attesting to its high immunogenicity compared with other subtypes of breast cancer. The increase in ongoing clinical trials investigating checkpoint inhibitors for the treatment of TNBC, reflects a great interest in finding effective therapies. However, in the case of metastasis, the efficacy of these agents is limited and may not prevent death.[3]

CD45 is a transmembrane protein tyrosine phosphatase receptor type C expressed exclusively in leukocytes, with opposing effects on T-cell receptor (TCR) activity.[4,5] Our group recently reported a new mechanism whereby TNBC inhibits the CD45 molecular pathway involving the Src family of tyrosine kinases, weakening TCR activity and resulting in tumor escape. An immune modulating peptide (C24D) that binds to CD45 receptors on immunosuppressed leukocytes was found to reactivate the immune response and lead to specific tumor cell killing.[6,7]

Galectin 3 (Gal3) is a protein found in breast cancer cells. It plays a role in the metastasis and evasion of immune surveillance through the killing of activated T cells.[8,9] Extracellular Gal3 induces T-lymphocyte apoptosis by binding to CD45, while intracellular Gal3 inhibits the apoptotic process by binding to the bcl-2 protein.[10] Gal3 downregulates TCR expression and interferon gamma (IFN-γ) secretion in both CD4 and CD8 T cells.[11] Emphasis has been placed on CD8 + T cells and their critical involvement in immunotherapy.[12]

A preliminary study by our group revealed that immune cells derived from patients with metastatic TNBC overexpress genes involved in the tumor secretion of small extracellular vesicles (sEVs, exosomes). sEVs contain proteins involved in immunosuppression.[13] EVs are enclosed in a flat or spherical phospholipid bilayer membrane, ranging from 30 to 150 nm in diameter. They contain biologically active molecules, such as DNA, RNA, lipids and proteins, that significantly contribute to intercellular communication and reprogramming of the tumor microenvironment and impede the effective response to cancer immunotherapy.[14,15] Our first thought was that Gal3 is expressed by sEVs like in hepatocellular carcinoma to induce immunosuppression by a possible mechanism involving integrin/FAK/SRC pathway.[16]

CONTACT Annat Raiter araiter@tauex.tau.ac.il Felsenstein Medical Research Center; Sackler Faculty of Medicine, Tel Aviv University, Petach Tikva, Israel; Rinat Yerushalmi rinaty@clalit.org.il Institute of Oncology, Davidoff Cancer Center, Rabin Medical Center, Petach Tikva, Israel
Supplemental data for this article can be accessed online at https://doi.org/10.1080/2162402X.2023.2246322

The study aimed to highlight TNBC-mediated immune evasion in order to identify ways to exploit the CD45 pathway as a novel strategy for effective targeted immunotherapy. Thus, we evaluated the association of Gal3 with tumor-derived sEVs in the induction of immunosuppression through the CD45 receptor.

Material and methods

Cell lines and cultures

Breast cancer cell lines MDA-MB-231, MCF7, BT474 and the normal breast cell line MCF-10A, were obtained from the ATCC and cultured following ATCC instructions. A large stock of cells was prepared to maintain their homogeneity and tumorigenicity. Cells were not used beyond passage 5 and were examined for mycoplasma (Mycoplasma Detection Kit, Biological Industries) at least once every 6 months.

Isolation of peripheral blood mononuclear cells (PBMCs)

PBMCs were isolated from the blood of ten healthy adult female donors obtained from the Blood Bank of Israeli National Blood Services, Magen David Adom. Samples were isolated by Ficoll – Hypaque density gradient centrifugation (Ficoll-Paque Plus, GE Healthcare). PBMCs were incubated in a complete RPMI medium supplemented with 5% human serum type AB.

Plasma from ten treatment-naïve patients with metastatic TNBC was obtained from the Davidoff Cancer Center of the Rabin Medical Center. All samples were procured according to the protocol approved by the Institutional Review Board of the Rabin Medical Center (0667–14-RMC).

Isolation of EVs from cell cultures and plasma of patients and healthy volunteers

The isolation and characterization of sEVs were performed by ultracentrifugation, according to the MISEV2018 guidelines.[17] Appropriate culture and harvesting conditions, such as the cell passage number and seeding confluence, were used for vesicle isolation. The sEVs isolated from MDA-MB-231 cells (tumor-derived exosomes, TEX) and MCF10-A cells (EX) were used in subsequent experiments. sEVs derived from plasma were purified using a similar procedure.

Characterization of sEVs

The presence of protein markers specific to sEVs, namely CD81, CD9 and CD63, was determined by fluorescence-activated cell sorting (FACS) analysis. sEVs (40 µl:48 × 10^7) were incubated with 4 µm aldehyde/sulfate latex beads 4% w/v (Invitrogen) according to the manufacturer's instructions. sEV-depleted fetal bovine serum (FBS) was added to the isolated sEVs. Anti-human CD81-APC, anti-human CD63-APC, anti-human CD9-APC and isotype control IgG1-APC (Miltenyi Biotec) antibodies were added to the samples for 30 minutes. The samples were run on a Navios flow cytometer, and the data were analyzed using Kaluza software (Beckman Coulter).

The concentration and particle size distribution of the purified sEVs were determined using a NanoSight NS300 nanoparticle tracking analyzer (Malvern Panalytical), equipped with a 405 nm laser. Once properly diluted, each sample was tracked for 60 seconds with the detection threshold set at the maximum. The vesicle size distribution and estimated concentration of nanoparticle tracking analysis (NTA) profiles were obtained from the given raw data files.

To confirm the characterization of sEVs, the sEV suspension (10 µl) was diluted, fixed in 2% paraformaldehyde, adsorbed on formvar/carbon-coated electron microscopy grids for 20 minutes, stained with 2% aqueous uranyl acetate for 5 minutes and washed with DDW. The samples were examined using a JEM 1400plus transmission electron microscope (Jeol, Japan).

Proteomics in exosomes by mass spectrometry

sEVs derived from MDA-MB-231 and MCF10-A cells and plasma from healthy donors and TNBC patients underwent mass spectrometry at the Smoler Proteomic Center (Technion, Haifa). The proteins were cleaved with trypsin and analyzed by LC-MS/MS using a QE HF mass spectrometer (Thermo Scientific). The data were identified using MaxQuant 1.5.2.8, against UniProt and decoy databases, to determine the false discovery rate. Statistical analyses were performed using the Perseus software. Missing proteins were imputed at 17 (log2). The identified proteins were filtered with an FDR < 0.01. The log2 intensities can be observed in the label-free quantification (LFQ)-normalized intensities.

Identification of sEVs expressing Gal3 binding protein (Gal3BP)

FACS analysis was performed using anti-CD81-APC, CD9-FITC (Miltenyi Biotec) and anti- Gal3BP (Novus Biological) antibodies, as described above.

Western blot identification of Gal3BP/Gal3 complex on sEVs

Isolated sEVs (27 × 10^7) were centrifuged and resuspended in 40 µL of RIPA buffer followed by a 20-minute freeze-thaw cycle. sEVs were harvested and centrifuged at 14,000 rpm (15 minutes at 4 °C). The supernatant was transferred to a new microtube for precipitation. Cell protein (50 µg/200 µl lysis buffer) from TEX or EX were incubated with 15 µg biotinylated anti-Gal3BP for 1 hour at 4°C with constant shaking. The complex was precipitated using streptavidin magnetic beads (µMACS Streptavidin Kit; Miltenyi Biotec) and placed in a microcolumn under the magnetic field of a µMACS separator. The column was rinsed and the target molecules that bonded to the biotinylated probe were eluted. The eluted samples were subjected to SDS-PAGE on a 10% gel. Western blotting was performed using anti-mouse Gal3BP (2 µg/ml; Novus Biological) or biotinylated Gal3 (0.1 µg/ml; R&D Systems),

followed by incubation with goat anti-mouse 680RD (Li-Cor) or streptavidin 800CW (Li-Cor) for 2 hours at room temperature. After washing, proteins were visualized using a Li-Cor Odyssey infrared imager. The data were normalized to anti-β-actin (R&D Systems) to determine the percentage of protein expression.

Physical interactions between Gal3BP and Gal3

A protocol was developed based on previously published protein-protein interaction protocols.[18] In brief, a 96-well plate was coated with recombinant Gal3BP 0.5 µg/ml overnight at 4°C. The plate was washed with 0.05% Tween-20 in PBS and blocked with 1% BSA and 0.05% Tween-20 in PBS at room temperature for one hour. The plate was washed and Gal3 containing supernatants of TEX and TNBC plasma or EX and plasma from healthy women (100 µl/well) were added (in progressive dilutions) for 2 hours at room temperature or overnight at 4°C. After intensive washing, anti-Gal3 biotinylated antibody (2 µg/ml) was added for one hour at room temperature, followed by streptavidin-HRP for another hour. Substrate solution (100 µl/well) was added for 30 minutes at room temperature. The stop solution (HCl 1 M) was added before the plate read at 450 nm.

FACS analysis for identification of Gal3BP/Gal3 complex on PBMCs

Leukocytes (1×10^6) were incubated with EX or TEX for 48 hours and GW4869 (10 µM; Sigma-Aldrich) and CD45 inhibitor (2.9 µM; Calbiochem) were added. GW4869 (CAS 6823-69-4) is an inhibitor of exosome biogenesis/release. The CD45 inhibitor (CAS 345,630-40-2, 2.9 µM; Calbiochem) is a PTPase CD45 inhibitor and a CD45 blocking peptide.[19]

Cells were transferred to FACS tubes and stained with anti-CD3-PC5.5 (Beckman Coulter), anti-Gal3-PE (R&D Systems), anti-mouse Gal3BP (Novus Biologicals) and mouse anti-human FITC (Jackson ImmunoResearch).

Detection of co-localization of Gal3/Gal3BP complex on T cells by confocal microscopy

PBMCs previously incubated with EX or TEX for 24 hours were transferred to cover slides using Cytospin 4 (Thermo Fisher Scientific). The cells were fixed with paraformaldehyde 4% for 10 minutes and washed with PBS-0.05% Tween 20. The slides were blocked with 1% bovine serum albumin (BSA) and 0.02% NaN_3 in PBS for 20 minutes at room temperature. After washing, anti-CD3-APC (Beckman Coulter) and biotinylated-anti-Gal3 antibody were added, followed by streptavidin-PE, anti-Gal3BP and anti-mouse FITC for 40 minutes at room temperature. DAPI (Invitrogen) was added to the slides, followed by washing and mounting (Electron Microscopy Sciences). Cells and cellular components, as well as intercellular reactions, were observed using a TCS SP5 confocal laser-scanning microscope (Leica Microsystems). High-resolution images (2048 pixels wide and 1536 pixels high) were captured using a Nikon camera. All images were magnified by a factor of 40. Pictures were taken from five different slides. For colocalization of CD9, Gal3BP and Gal3, CD3 was replaced by anti-CD9 (MACS).

FACS analysis for identification of activated and suppressed immune cells

Leukocytes (1×10^6) were incubated with EX or TEX, and GW4869 (10 µM), CD45 inhibitor (2.9 µM) and the cell activator (ImmunoCult Human CD3/CD28/CD2, StemCell Technologies) were added for 72 hours. Then, lymphocytes were extracted from the co-cultures, centrifuged and resuspended in PBS for FACS analysis. PBMCs (0.5×10^6/50 µl PBS) were incubated with the following antibodies for multicolor staining for 40 minutes at room temperature: CD3-PC5.5, CD4- PC7, CD8-KO, CD56-PE, CD69, CD57 and CD25 (Beckman Coulter). The cells were then washed twice for 10 minutes (1200 rpm, 4°C). To determine intracellular FoxP3 expression, cells were treated with permeabilization buffer (R&D Systems).

Cytokines

Levels of human IFNγ and IL-10 were determined with ELISA Ready SET-Go (eBioscience) and Quantikine ELISA Human IL-10 KIT (R&D Systems). Human IL-35 was determined with ELISA using kits from Elabscience Biotechnology following manufacturer instructions.

Statistical analysis

The results are presented as mean±standard deviation (SD) or standard error (SE). To determine whether the data from the test samples were significantly different from those of the control samples, two-tailed students' t-tests were performed using GraphPad software. Analysis of variance (ANOVA) was used for multiple comparisons. Statistical significance was defined as $p < 0.05$.

Results

Isolation and characterization of sEVs

The experimental procedures for the isolation and characterization of sEVs were adjusted and standardized as described in Material and Methods.[17] The isolated sEVs were characterized by morphological, dimensional and biomolecular parameters.

FACS analysis was used to evaluate the expression of three receptors, CD81, CD63 and CD9, in sEVs derived from MDA-MB-231 cells, normal breast MCF10-A cells. The expression of the three receptors was evaluated in sEVs from plasma of patients with TNBC and compared to sEVs from the plasma of healthy female volunteers (Figure 1a, Figure S1). A representative histogram showing the distribution of the sEVs and the expression of each of the receptors in the different samples is shown in Figure 1b. Overall, CD81 was expressed by more than 90% of sEVs evaluated, with no significant differences among samples. CD63 was expressed by 8.1 ± 1.6% of sEVs derived from MDA-MD-231 cells and a significantly lower percentage of sEVs from the other sources

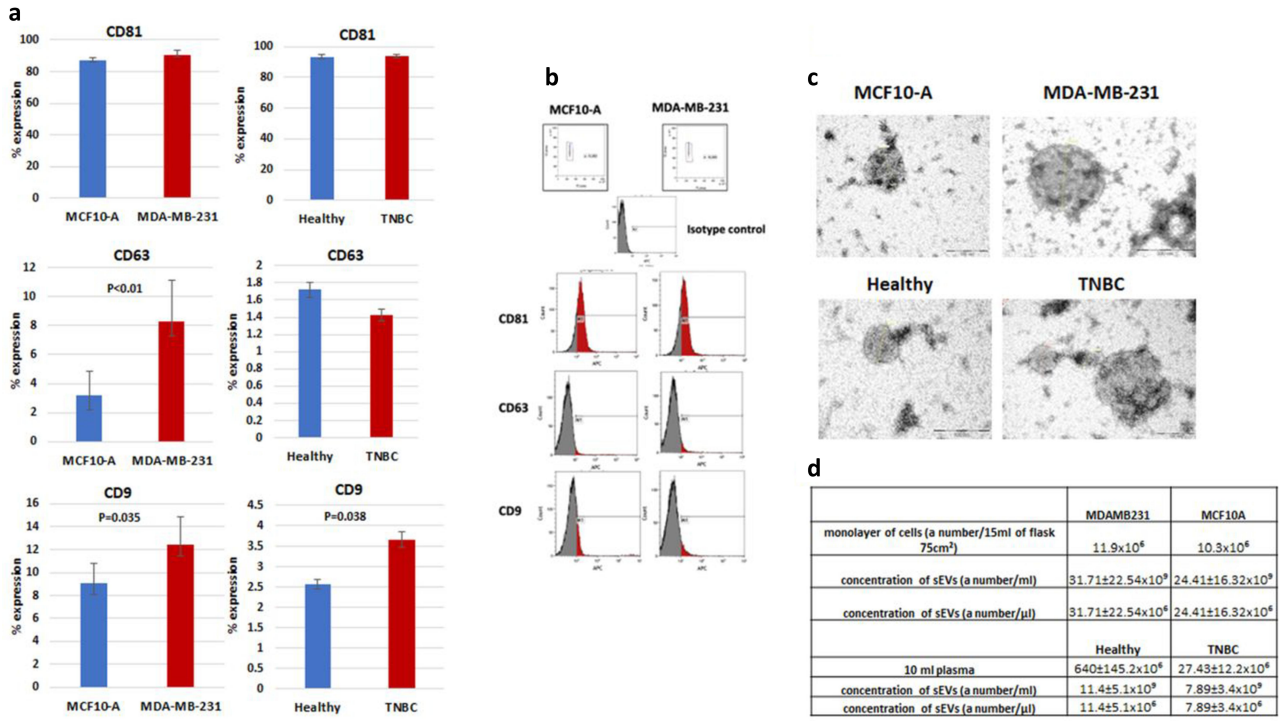

	MDAMB231	MCF10A
monolayer of cells (a number/15ml of flask 75cm²)	11.9×10^{6}	10.3×10^{6}
concentration of sEVs (a number/ml)	$31.71\pm22.54\times10^{9}$	$24.41\pm16.32\times10^{9}$
concentration of sEVs (a number/µl)	$31.71\pm22.54\times10^{6}$	$24.41\pm16.32\times10^{6}$
	Healthy	TNBC
10 ml plasma	$640\pm145.2\times10^{6}$	$27.43\pm12.2\times10^{6}$
concentration of sEVs (a number/ml)	$11.4\pm5.1\times10^{9}$	$7.89\pm3.4\times10^{9}$
concentration of sEVs (a number/µl)	$11.4\pm5.1\times10^{6}$	$7.89\pm3.4\times10^{6}$

Figure 1. Characterization of isolated sEVs. a. FACS analysis showing the expression of CD81, CD63, and CD9 in sEVs isolated from MDA-MB-231 cells compared to MCF10-A cells (n = 6) and from plasma of TNBC patients compared to plasma of healthy female volunteers (n = 10) Results are expressed as mean±SE; *p* values are shown in the figure (ANOVA). b. Gated small vesicles (a) discarding debris. Representative histogram showing the distribution of sEVs. In red, positive for CD81, CD63 and CD9 in TNBC derived sEVs. In blue, CD81, CD63 and CD9 positives sEVs derived from healthy or normal breast cells. Isotype control (IgG1-APC) c. Morphology and size of isolated sEVs assessed with transmission electron microscopy. Scale bar = 100 nm. D. NTA results of sEVs isolated from 10×10^6 cells or from 10 ml plasma derived from one sample of each of the sources.

($p < 0.01$). CD9 was expressed by 12.8 ± 2.4% of sEVs from MDA-MB-231 cells compared to 5.9 ± 1.7% of sEVs from MCF10-A cells ($p = 0.035$). CD9 was also expressed by 3.7 ± 0.4% of sEVs from plasma of patients with TNBC compared to 2.5 ± 0.47% of sEVs from plasma of healthy volunteers ($p = 0.038$).

The sEV diameter (40–200 mm) and typical rounded structure (Figure 1c) were determined by transmission electron microscopy for all samples. The sample for transmission electron microscopy was diluted to obtain one vesicle per picture. In sEVs derived from healthy volunteers or from TNBC patients more that one sEV is observed. No differences in size were detected in the different samples. Confirmation of the FACS and transmission electron microscopy was assessed by NTA. The vesicle size distribution and estimated concentration by NTA were obtained from available raw data files and are shown in Figure 1d.

sEVs contain Gal3BP

Following the validation and quantification of sEVs based on the positive expression of CD81, CD63 and CD9 (Figures 1a & 1b), mass spectrometry analysis was performed on isolated sEVs from the four groups: sEvs derived from MCF10-A (EX), MDA-MB-231 (TEX), healthy women volunteers' plasma (Healthy) and plasma of TNBC patients (TNBC). Of the 340 proteins identified, 23 that were found in at least 8/12 samples, were selected for evaluation (Table S1). The remaining 317 proteins were found only in one or two samples, therefore, they are not included in the analysis. The Venn diagram showing 23 identified proteins found in at least 8/12 samples is presented in Figure 2a.

Mass spectrometry analysis revealed that 43.5% of the 23 identified proteins were expressed by all four groups. Only 8.7% of the identified proteins were found in EX (sEVs from MCF10-A cells and from healthy control plasma), and 39.1% were found exclusively in TEX (sEVs from MDA-MB-231 cells and plasma from patients with TNBC). The remaining 8.7% of the proteins were found in a few samples in each group. TNBC-cell-secreted Gal3BP was identified in samples of 4 of the 5 patients and in the MDA-MB-231 samples in contrast to other proteins that were found only in a few of the TNBC samples. Gal3BP, identified via mass spectrometry, is annotated in the ExoCarta database as an sEV (exosome) marker (Table S1).

The percentage of CD9+ sEVs was significantly higher in TEX than EX: 30.25 ± 5.4% versus 3.25 ± 0.8 of the vesicles, respectively ($p = 0.035$). The corresponding rates for Gal3BP were 10.25 ± 1.5% and 1.15 ± 0.5% ($p = 6.6 \times 10^{-05}$) (Figure 2b). Figure 2c presents a representative dot plot obtained from FACS analysis showing the double staining of CD9/Gal3BP in TEX and EX.

Gal3BP forms a complex with secreted Gal3

Gal3 has been shown to be expressed at higher levels in tumors compared to normal cells.[20] Thus, the first step to determine

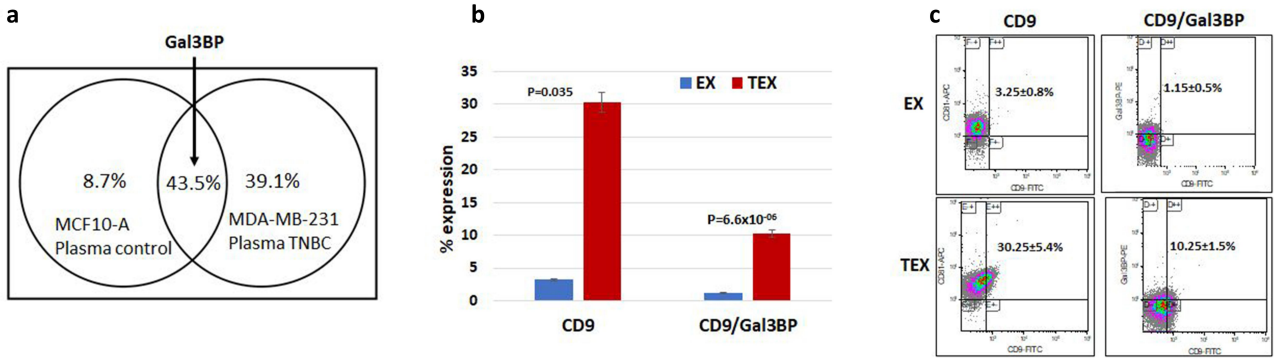

Figure 2. Expression of GalBP by TEX. a. Venn diagram depicting the percentage of 23 selected proteins revealed by mass spectrometry analysis that were expressed or contained by sEVs isolated from MDA-MB-231 and MCF10-A cells and in plasma of healthy volunteers and TNBC patients. Gal3BP as part of the 43.5% proteins expressed of the 23 selected proteins, was found in the samples from the TNBC groups. b. Bars showing the percentage of CD9 expression and $CD9^+/Gal3BP^+$ identified on sEVs isolated from normal breast cells (EX) or from TNBC cells (TEX). Results are expressed as mean±SD (n = 5); *p* values are shown in the figure (two-tailed t test). c. Representative dot blot showing double stained $CD9^+/Gal3BP^+$ in TEX vs EX by FACS analysis.

the connection between Gal3BP and TNBC was to measure Gal3 secretion by three breast cancer cell lines: MDA-MB-231, MCF7, BT474 and normal breast cells. Measurement of Gal3 secretion in MDA-MB-231 cells yielded a fivefold higher value than in two other breast cancer cell lines (MCF7 and BT474) and normal breast cells ($p < 0.003$) (Figure 3a). Then, we compared secreted Gal3 in plasma of TNBC patients to plasma of healthy women. The Gal 3 in plasma of TNBC yielded a 1.9-fold higher value than in plasma of healthy women ($p = 0.001$) (Figure S1).

Then, we aim to demonstrate that the secreted Gal3 interacts with Gal3BP. An assay was then designed to evaluate the physical interactions between Gal3BP and Gal3 (Figure 3b) using recombinant Gal3BP and secreted Gal3. Gal3BP/Gal3 interactions were significantly higher for the TEX samples. Gal3 derived from TEX binds to the recombinant Gal-3BP and results generated a linear curve shape depending on the sample dilution (Figure 3c).

To confirm the binding of the secreted Gal3 to Gal3BP expressed by EX and TEX to form a complex, western blot

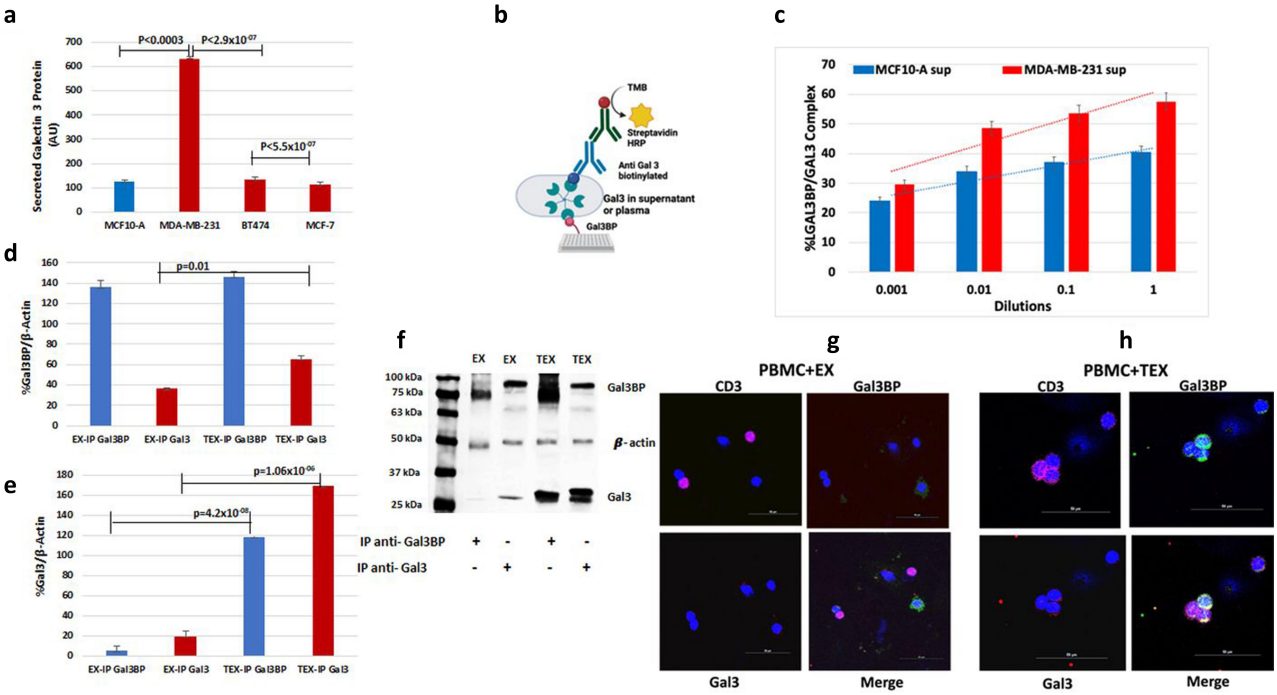

Figure 3. Formation of a complex of Gal3BP with Gal3. a. Gal3 secretion by MDA-MB-231, MCF10-A, ER+ MCF-7, and Her2+ BT474 cells. Results are expressed as mean ±SD (n = 3) (two-tailed t test). b. An assay was developed to evaluate the physical interactions between Gal3BP and Gal3. c. Bars showing a linear curve shape, depending on the sample dilution. Significantly higher physical interactions between Gal3BP and Gal3 derived from MDA-MB-231 and plasma of TNBC patients cells compared to MCF10-A or plasma of healthy women in triplicate ($p < 0.007$). Results are expressed as mean±SD (two-tailed t-test). d. Percentage of Gal3BP protein in TEX and EX immunoprecipitated with either anti-Gal3BP or anti-Gal3 antibodies (n = 3). Results are expressed as mean±SD; *p* values are shown in the figure (two-tailed t test). e. Percentage of Gal3 protein in TEX or EX immunoprecipitated with either anti Gal3BP or anti Gal3 antibodies (n = 3, mean±SD) (2-tailed t test). f. Western blot analysis showing expression of Gal3 only in TEX immunoprecipitated with anti-Gal3BP. Gal3BP expression was found in EX or TEX immunoprecipitated with anti-Ga3BP. Immunoprecipitation with anti-Gal3, resulted in higher Gal3BP expression in TEX than in EX. g. Immunofluorescence of PBMCs treated with EX. CD3 (purple) expressing Gal3BP (green)/Gal3 (red) complex in EX. Scale bar = 50 µm. H. Immunofluorescence of PBMCs treated with TEX. Triple staining of Gal3BP/Gal3 complex on CD3 cells (yellow). Pictures taken under confocal microscope, nucleus stained with DAPI (blue), Scale bar = 50 µm.

analysis was performed. Immune precipitation with anti-Gal3BP yielded a band (Gal3BP = 80 KDa) in both EX and TEX (136.0 ± 6.6% vs 146.2 ± 4.0% respectively, $p = 0.1$). In the immune-precipitated Gal3BP, Gal3 (30 KDa band) was found exclusively in TEX (118.6 ± 1.7% vs 5.0 ± 0.6 in EX, $p = 4.2 \times 10^{-08}$). As a result of immune precipitation with anti-Gal3, Gal3BP was higher in TEX than EX (65.3 ± 3.06% vs 36.2 ± 0.9%, $p = 0.01$). Gal 3 was higher in TEX (168.7 ± 5.3 vs 19.2 ± 0.31%, $p = 1.06 \times 10^{-06}$) (Figures 3d–f). The results validate the presence of Gal3BP/Gal3 complex in TEX.

Confocal immunofluorescence microscopy was used to analyze whether Gal3 (red) was associated with Gal3BP (green), and whether Gal3 and Gal3BP were associated with the CD3 receptor (purple). Triple staining (yellow) of CD3 with Gal3BP and Gal3 was observed in PBMCs incubated with TEX. In contrast, the PBMCs incubated with EX resulted in negligible overlap (Figures 3g, h). The majority of these localized structures were positive for CD9 receptors on sEVs (Figure S2).

Gal3BP/Gal3 complex regulates the CD45 receptor pathway on leukocytes

FACS analysis showed that the binding of Gal3BP and Gal3 to PBMCs incubated with TEX was significantly inhibited in cells previously blocked with a CD45 peptide. TEX added to PBMCs showed double staining for Gal3B/Gal3 binding to gated CD45 + cells: 28.25 ± 4.6% compared to 16.25 ± 1.3% in EX-treated cells ($p = 0.02$). Blocking the CD45 receptor significantly inhibited the binding of both proteins in TEX-treated cells ($p = 0.005$) (Figures 4a, b). The addition of GW4869, an inhibitor of sEV biogenesis/release (to neutralize the effect of PBMC-secreted sEVs), did not affect CD45 blocking in TEX-treated PBMCs (Figure S3).

The next step was to determine whether the complex down-regulated the CD45 molecular pathway. A 2.5-fold increase in Lck Y505 phosphorylation was observed in PBMCs treated with TEX and the Gal3/Gal3BP complex ($p < 0.05$) and compared to that in EX-treated PBMCs. Phosphorylation of Lck Y394 was 1.5-fold higher in TEX-treated PBMCs than in EX-treated PBMCs ($P = 0.034$). The addition of the complex to the cells reduced Lck Y394 phosphorylation, but not significantly, compared to EX. ZAP Y493 phosphorylation was significantly reduced with the addition of TEX (15.9 ± 4.6%) or complex (11.53 ± 6%) compared to EX (29.5 ± 4.2) ($p < 0.05$); the same pattern was observed for VAV-1 ($p < 0.04$) (Figure 4c). We found that addition of TEX to PBMCs resulted in an increase in the phosphorylation of the tyrosine (Y) 505 in the Lck tyrosine kinase and a decrease in the phosphorylation of the Y394 in the Lck, causing inhibition of Lck. Additionally, we found a decrease in the phosphorylation of the Y493 in the ZAP70 protein kinase and in the Y178 in VAV-1 resulting in TCR de-activation. A representative FACS histogram is shown in Figure 4d.

Gal3BP/Gal3 complex induces immunosuppression through CD45 receptor on T cells

To assess if T-regulatory (Treg) cells are involved in the immunosuppression exerted by the Gal3BP/Gal3 complex, PBMCs were incubated with either EX, TEX or Gal3BP/Gal3 complex

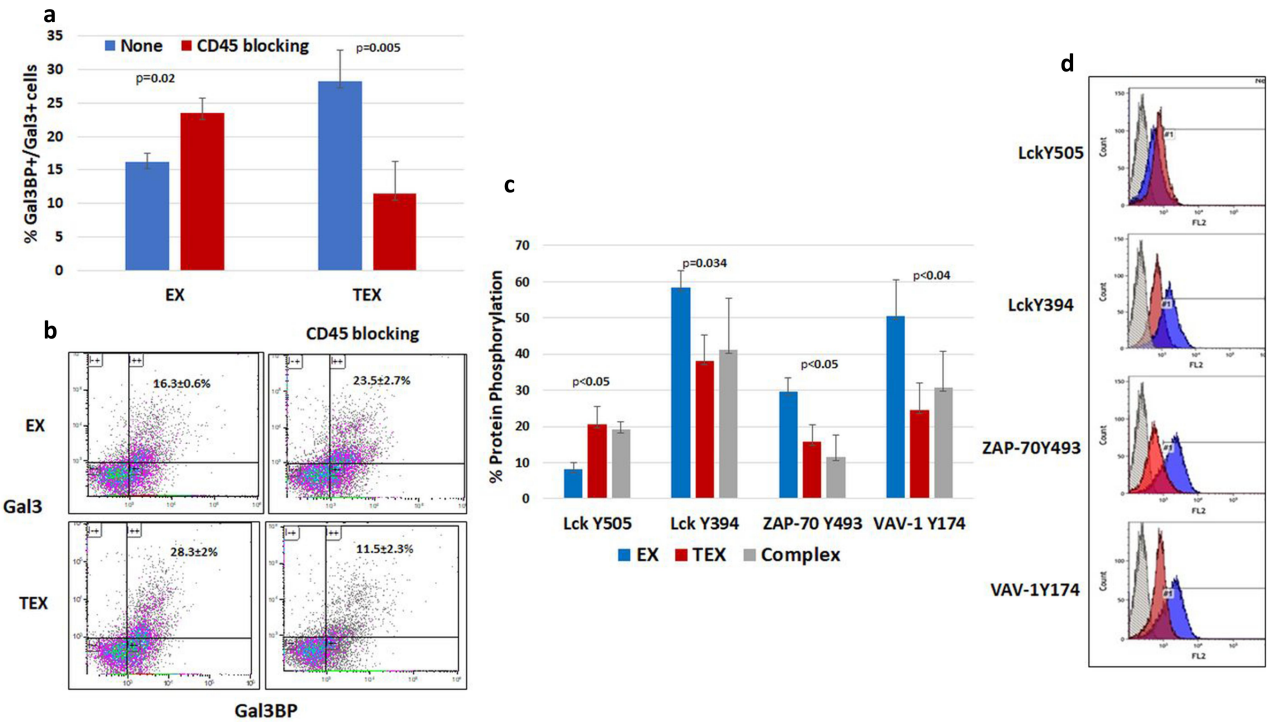

Figure 4. Gal3/Gal3BP complex binding to CD45 and inhibiting CD45 signaling pathway in TEX. A. Percentage of T cells displaying Gal3BP/Gal3 complex with and without CD45 blocking in EX- and TEX-treated cells ($n = 3$). Results are expressed as mean±SD (two-tailed t test). B. Representative dot blot of FACS analysis of CD3+ gated cells expressing Gal3BP/Gal3 complex. C. Percentage of Lck Y505, Lck Y394, ZAP-70 Y493 and VAV-1 Y174 phosphorylation in PBMCs treated with EX, TEX, or complex (Gal3BP and Gal3 recombinant proteins). D. Representative histogram showing phosphorylation of proteins in the CD45 pathway after treatment with EX (red) or TEX (blue).

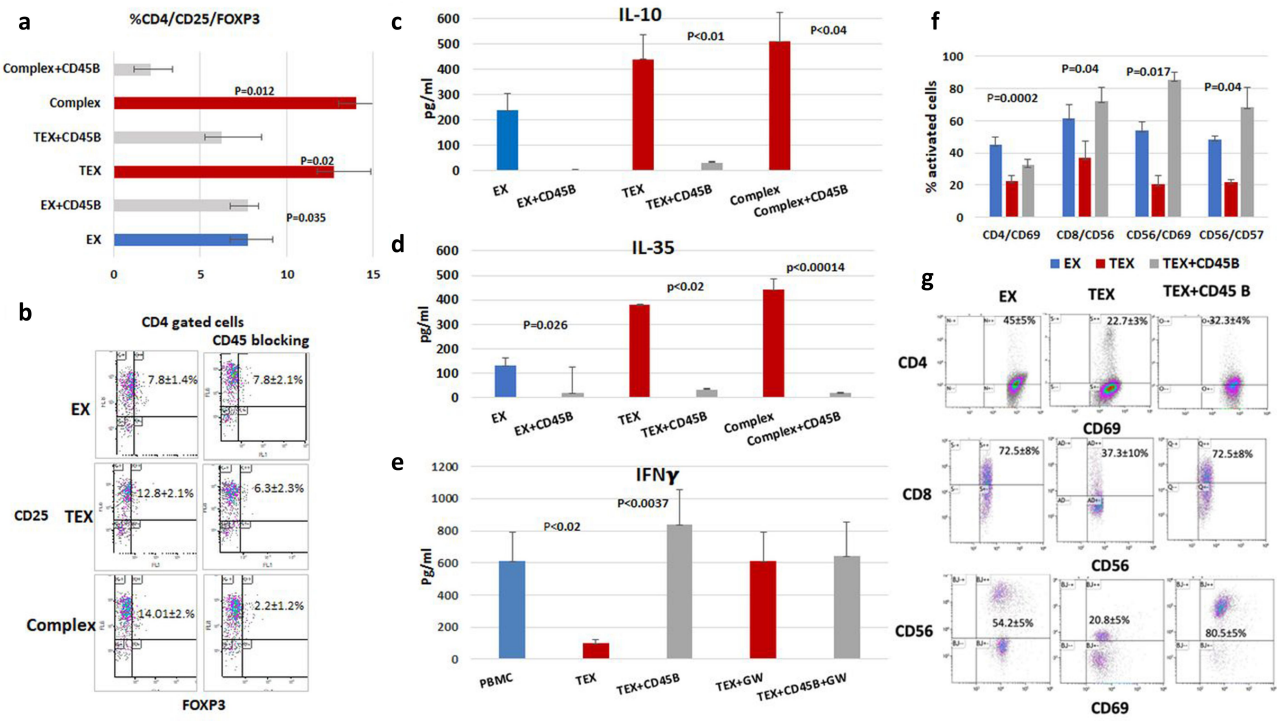

Figure 5. Effect of CD45 blocking on Gal3BP/Gal3 protein-induced immunosuppression. a. Percentage of Treg cells ($CD4^+/CD25^+FOXP3^+$) in PBMCs treated with EX compared to TEX or Gal3BP/Gal3 complex ± CD45 blocking. Results are expressed as mean±SE (n = 4) (*p* value by ANOVA). b. Representative dot blot of FACS data showing percentage gated CD4 cells expressing CD25-APC and FOXP3-FITC (Treg cells) in EX- or TEX-treated cells. c. IL-10 and IL-35 were detected in supernatants of PBMCs treated with either TEX or EX from the different experiments. IL-10 secretion by cells. Results are expressed as mean±SE (n = 6) (*p* value by ANOVA). d. IL-35 secretion by cells. Results are expressed as mean±SE (n = 7); (*p* values by ANOVA). e. IFNγ secretion of lymphocytes incubated with TEX or TEX+GW4869 (an inhibitor of exosome secretion) and with/without CD45 blocking. f. Percentage of activated T and NK cells after incubation of lymphocytes with EX or TEX with/without CD45 blocking. Results are expressed as mean±SE (n = 4); *p* values by ANOVA). g. Representative dot blot of FACS data.

(Figure 5a) and the percentage of CD4+/CD25+/FOXP3+ (Treg) cells was determined by FACS analysis.

Extracellular Gal3 is known to induce T lymphocyte apoptosis via stimulation of CD45[20]. Therefore, the next phase of the study was aimed at validating Gal3BP/Gal3-complex induction of immunosuppression through the CD45 molecular pathway.

FACS analysis showed that the percentage of T regulatory (Treg) cells increased significantly when PBMCs were incubated with TEX or Gal3BP/Gal3 complex compared to EX ($p = 0.04$; Figures 5(a, b). Blocking the CD45 receptor leads to the depletion of Treg cells. The percentage of CD4+/CD25+/FOXP3+ (Treg) decreased from 12.8 ± 2.5% to 6.25 ± 2.3% in the TEX-treated PBMCs ($p = 0.02$) and to 6.0 ± 1.2% in the complex-treated PBMCs ($p = 0.012$).

According to the percentage of Treg after addition of TEX or the complex to PBMCs, a significant increase of the immunosuppressive IL-10 and IL-35 cytokines was observed, compared to the addition of EX ($p < 0.01$, and $p < 0.02$, respectively) (Figures 5c, d). Blocking CD45 drastically inhibited the secretion of IL-10 ($p < 0.004$) and IL-35 ($p < 0.00014$) in PBMCs treated with TEX or complex.

IFNγ secretion was inhibited when TEX was added to the PBMCs (Figure 5e). IFNγ levels in activated PBMCs incubated with EX were 6.1-fold higher than those in PMBCs incubated with TEX ($P = 0.02$). Blocking CD45 receptors in activated PBMCs restored IFNγ secretion ($p = 0.0004$). The addition of GW4869 had no effect on the cytokine secretion. Furthermore, we evaluated IFNγ secretion by activated PBMCs treated with sEVs isolated from plasma of TNBC patients. Compared to the effect of EVs derived from plasma of healthy women, those derived from TNBC patients significantly inhibited IFNγ secretion ($p = 0.0006$, Figure S4). Blocking the CD45 receptor in the activated PBMCs pre-treated with sEVs derived from plasma of TNBC patients recovers the levels of IFNγ similar to those secreted by PBMCs treated with sEVS derived from plasma of healthy women.

FACS analysis was used to identify the activated subpopulations recovered from immunosuppression exerted by TEX after CD45 blocking. Of the 11 leukocyte subpopulations analyzed, only 4 were activated after CD45 was blocked (Figure 5f). The percentage of CD4+/CD69+ cells, which decreased significantly with the addition of TEX ($p = 0.0002$), was restored from 22.75 ± 3 to 32.2 ± 3.8 ($p = 0.04$) after the CD45 blocking. The percentage of CD8+/CD56+ cells increased from 37.3 ± 10.2 after TEXtreatment to 72.5 ± 8.5 in CD45-blocked PBMCs ($p = 0.017$). In NK subpopulations, the percentage of CD56+/CD69 rose from 20.75 ± 5.5 with TEX treatment to 80.5 ± 5.2 in CD45 blocked cells ($p < 0.04$), and the percentage of CD56+/CD57+ rose from 21.6 ± 2.4 to 68.6 ± 12.3 ($p < 0.04$). A representative FACS dot plot of the four experiments is shown in Figure 5g.

Discussion

Innovative immunotherapeutic strategies are critical for TNBC because of its poor prognosis and resistance to conventional treatments.[3]

In a previous publication, we found that a novel peptide binding to CD45 on immunosuppressed lymphocytes reversed TNBC immunosuppression, resulting in specific tumor killing[6]. To elucidate this escape mechanism, we explored the involvement of potential molecules secreted by TNBC cells.

EVs secreted by tumor cells are involved in immune suppression as part of an immune escape mechanism.[21] We first separated and characterized isolated EVs from the plasma of patients with TNBC and from MDA-MB-231 cells using NTA, transmission electron microscopy and antibodies against three known EV receptors: CD81, CD63 and CD9.[22] The percentage of CD9 cells was significantly higher in both sEVs derived from MDA-MB-231 cells and patient plasma than in sEVs from normal breast cells and the plasma of healthy volunteers. CD9 on the surface of sEVs from breast cancer cells has been found to be essential for the uptake of sEVs by leukocytes, which become immunosuppressed.[23] The immunosuppressive activity of sEVs occurs in part via protein mediators of intercellular communication.[24] Using mass spectrometry, we identified Gal3BP in sEVs isolated from the plasma of patients and MDA-MB-231 cells. The level of Gal3BP expressed in $CD9^+$ sEVs from tumor cells was tenfold higher than that of sEVs from normal cells. Accordingly, a National Cancer Institute (NCI-60) proteomic study identified Gal3BP in sEVs derived from tumor cells as a cancer-specific biomarker,[25] and we found that those EVs expressed CD9. EVs associated with Gal3BP have been shown to serve as key regulators of cell – cell and cell-extracellular matrix crosstalk in metastatic breast cancer.[24,26] In contrast, a strong negative correlation was reported between the expression of Gal3BP and ErbB2 receptor, a known marker of aggressive progression and poor prognosis in breast tumors.[27] These findings are in line with a dual immunosuppressive/immunostimulatory role for Gal3BP, as suggested by previous studies. The addition of Gal3BP to the culture of human PBMCs suppressed the transcriptional activity and secretion of IL-4, IL-5 and IL-13 cytokines,[28,29] whereas Gal3BP contributed to the activation of $CD3^+$ T cell-mediated secretion of IL-2.[30] In a co-culture of lymphocytes with breast cancer cells, Gal3BP was identified as an IFN-inducible gene, enhancing the mRNA and protein secretion of IFNα, IFNβ and IFNγ.[31,32] Given these contradictory reports, we sought to clarify the involvement of Gal3BP in immunosuppression in TNBC by using peripheral lymphocytes from affected patients. We found Gal3BP in EX and also in TEX, however, Gal3 is mostly secreted by tumor cells. In this study we demonstrated one of the different functions exerted by Gal3BP bound to Gal3 as a complex, predominantly in TNBC, reduced the levels of IFNγ. We assumed that the secreted Gal3 may form a complex with Gal3BP in tumor-derived EVs, similar to the process in viral infections.[27,33] Some viruses, such as HIV, human T-cell leukemia virus (HTLV), Epstein – Barr virus (EBV) or Rift Valley fever virus (RVFV), have been reported to transmit viral proteins, nucleic acids or genomic RNA into recipient cells through EVs. EVs containing viral particles can be a strategy to evade the immune response.[34]

The immunosuppressive activity of the Gal3BP/Gal3 complex was demonstrated by an increase in the percentage of Treg cells in correlation with the immunosuppressive cytokines IL-10 and IL-35 when the complex was added to normal PBMCs.[35,36] We also demonstrated that the Gal3BP/Gal3 complex binds to CD45 in T cells and regulates the phosphorylation of proteins involved in the CD45 signaling pathway.[6] Blocking the CD45 receptor to prevent complex binding resulted in a decrease in the percentage of Treg cells and consequently, IL-10 and IL-35 secretion. At the same time, blocking CD45 significantly increased IFNγ secretion and the percentage of CD4+/CD69+, CD8+/CD56+ and CD56+/CD69 + activated effector cells[37] (Figure 6).

Together, these findings confirm that the interaction between the CD45 receptor and Gal3BP/Gal3 complex is an essential factor in tumor immunosuppression. There is a large amount of data in the literature on the involvement of Gal3BP and Gal3 in breast cancer, but the roles described for both are

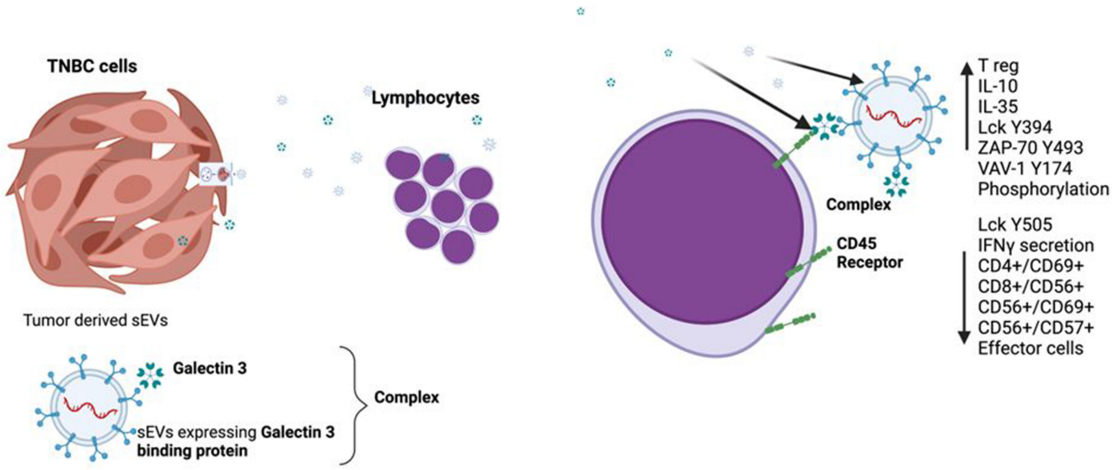

Figure 6. A new TNBC immunosupressive mechanism. Gal3BP/Gal3 complex secreted by TNBC cells induces immunosuppression through the CD45 receptor on T cells.

contradictory. Moreover, the immunosuppressor mechanisms have not been completely elucidated. In this study, we describe a different mechanism exerted by Gal3BP and Gal3 complex that acts via the CD45 receptor on T cells.[38] We suggest this mechanism as an immunosuppression mechanism used by TNBC to escape the immune system, specifically in peripheral leukocytes.[27,39]

This manuscript expresses the importance of the immune-suppression of peripheral blood lymphocytes, which may imply a predictive and prognostic significance in TNBC patients.

TNBC is a highly complex, heterogeneous disease with high probability of disease recurrence and rapid disease progression, despite adequate systemic treatment. Immunotherapy has emerged as an important modality in TNBC treatment. However, clinical results indicate that only a small proportion of patients with TNBC actually benefit from immunotherapy.

This finding has important implications for the development of a promising targeted strategy to improve clinical outcomes in patients with TNBC and to treat non-responders to existing treatments.

Disclosure statement

No potential conflict of interest was reported by the author(s).

Funding

This study was partially funded by the Berlinski Foundation, Israel-USA (N/A).

ORCID

Annat Raiter http://orcid.org/0000-0001-7357-1662

Data availability statement

All data relevant to the study are included in the article or are uploaded as supplementary information. Additional data are available on request.

Ethics approval and consent to participate:

All samples were procured according to the protocol approved by the Institutional Review Board of Rabin Medical Center (0667–14-RMC).

References

1. Liu C, Li Y, Xing X, Zhuang J, Wang J, Wang C, Zhang L, Liu L, Feng F, Li H, et al. Immunogenomic landscape analyses of immune molecule signature-based risk panel for patients with triple-negative breast cancer. Mol Ther Nucleic Acids. 2022;28:670–684. doi:10.1016/j.omtn.2022.04.034.
2. Howard FM, Pearson AT, Nanda R. Clinical trials of immunotherapy in triple-negative breast cancer. Breast Cancer Res Treat. 2022;195(1):1–15. doi:10.1007/s10549-022-06665-6.
3. Valencia GA, Rioja P, Morante Z, Ruiz R, Fuentes H, Castaneda CA, Vidaurre T, Neciosup S, Gomez HL. Immunotherapy in triple-negative breast cancer: a literature review and new advances. World J Clin Oncol. 2022;13(3):219–236. doi:10.5306/wjco.v13.i3.219.
4. Al Barashdi MA, Ali A, McMullin MF, Mills K. Protein tyrosine phosphatase receptor type C (PTPRC or CD45). J Clin Pathol. 2021;74(9):548–552. doi:10.1136/jclinpath-2020-206927.
5. Courtney AH, Shvets AA, Lu W, Griffante G, Mollenauer M, Horkova V, Lo W-L, Yu S, Stepanek O, Chakraborty AK, et al. CD45 functions as a signaling gatekeeper in T cells. Sci Signal. 2019;12(604):eaaw8151. doi:10.1126/scisignal.aaw8151.
6. Raiter A, Zlotnik O, Lipovetsky J, Mugami S, Dar S, Lubin I, Sharon E, Cohen CJ, Yerushalmi R. A novel role for an old target: CD45 for breast cancer immunotherapy. Oncoimmunology. 2021;10(1):1929725. doi:10.1080/2162402X.2021.1929725.
7. Alon D, Paitan Y, Robinson E, Ganor N, Lipovetsky J, Yerushalmi R, Cohen CJ, Raiter A. Downregulation of CD45 signaling in COVID-19 patients is reversed by C24D, a novel CD45 targeting peptide. Front Med. 2021;8:675963. doi:10.3389/fmed.2021.675963.
8. Fukumori T, Takenaka Y, Yoshii T, Choi Kim H-R, Hogan V, Inohara H, Kagawa S, Raz A. CD29 and CD7 mediate Galectin-3-Induced type II T-Cell apoptosis. Cancer Res. 2003;63:8302–8311.
9. Ruvolo PP. Galectin 3 as a guardian of the tumor microenvironment. Biochimica et Biophysica Acta (BBA). 2016;1863:427–437. doi:10.1016/j.bbamcr.2015.08.008.
10. Chen HY, Fermin A, Vardhana S, Weng I-C, Lo KFR, Chang E-Y, Maverakis E, Yang R-Y, Hsu DK, Dustin ML, et al. Galectin-3 negatively regulates TCR-mediated CD4+ T-cell activation at the immunological synapse. Proc Natl Acad Sci U S A. 2009;106(34):14496–14501. doi:10.1073/pnas.0903497106.
11. de Oliveira FL, Gatto M, Bassi N, Luisetto R, Ghirardello A, Punzi L, Doria A. Galectin-3 in autoimmunity and autoimmune diseases. Exp Biol Med (Maywood). 2015;240(8):1019–1028. doi:10.1177/1535370215593826.
12. Martinez-Bosch N, Vinaixa J, Navarro P. Immune evasion in pancreatic cancer: from mechanisms to therapy. Cancers Basel. 2018;10(1):6. doi:10.3390/cancers10010006.
13. Abhange K, Makler A, Wen Y, Ramnauth N, Mao W, Asghar W, Wan Y. Small extracellular vesicles in cancer. Bioact Mater. 2021;6(11):3705–3743. doi:10.1016/j.bioactmat.2021.03.015.
14. Gao Y, Qin Y, Wan C, Sun Y, Meng J, Huang J, Hu Y, Jin H, Yang K. Small extracellular vesicles: a novel avenue for cancer management. Front Oncol. 2021;11:638357. doi:10.3389/fonc.2021.638357.
15. Marar C, Starich B, Wirtz D. Extracellular vesicles in immunomodulation and tumor progression. Nat Immunol. 2021;22(5):560–570. doi:10.1038/s41590-021-00899-0.
16. Wang M, Tian F, Ying W, Qian X. Quantitative proteomics reveal the anti-tumour mechanism of the carbohydrate recognition domain of Galectin-3 in Hepatocellular carcinoma. Sci Rep. 2017;7(1):5189. doi:10.1038/s41598-017-05419-5.
17. Théry C, Witwer KW, Aikawa E, Alcaraz MJ, Anderson JD, Andriantsitohaina R, Antoniou A, Arab T, Archer F, Atkin-Smith GK, et al. Minimal information for studies of extracellular vesicles 2018 (MISEV2018): a position statement of the international society for extracellular vesicles and update of the MISEV2014 guidelines. J Extracell Vesicles. 2018;7(1):1535750. doi:10.1080/20013078.2018.1535750.
18. Al-Mugotir M, Kolar C, Vance K, Kelly DL, Natarajan A, Borgstahl GEO. A simple fluorescent assay for the discovery of protein-protein interaction inhibitors. Anal Biochem. 2019;569:46–52. doi:10.1016/j.ab.2019.01.010.
19. Baba M, Yong Ma B, Nonaka M, Matsuishi Y, Hirano M, Nakamura N, Kawasaki N, Kawasaki N, Kawasaki T. Glycosylation-dependent interaction of Jacalin with CD45 induces T lymphocyte activation and Th1/Th2 cytokine secretion. J Leukoc Biol. 2007;81(4):1002–1011. doi:10.1189/jlb.1106660.
20. Farhad M, Rolig AS, Redmond WL. The role of Galectin-3 in modulating tumor growth and immunosuppression within the tumor microenvironment. Oncoimmunology. 2018;7(6):e1434467. doi:10.1080/2162402X.2018.1434467.

21. Raimondo S, Pucci M, Alessandro R, Fontana S. Extracellular vesicles and tumor-immune escape: biological functions and clinical perspectives. Int J Mol Sci. 2020;21(7):2286. doi:10.3390/ijms21072286.
22. Doyle LM, Wang MZ. Overview of extracellular vesicles, their origin, composition, purpose, and methods for exosome isolation and analysis. Cells. 2019;8:727. doi:10.3390/cells8070727.
23. Ekström K, Crescitelli R, Pétursson HI, Johansson J, Lässer C, Olofsson Bagge R. Characterization of surface markers on extracellular vesicles isolated from lymphatic exudate from patients with breast cancer. Bmc Cancer. 2022;22(1):50. doi:10.1186/s12885-021-08870-w.
24. Shenoy GN, Bhatta M, Bankert RB. Tumor-associated exosomes: a potential therapeutic target for restoring anti-tumor t cell responses in human tumor microenvironments. Cells. 2021;10(11):3155. doi:10.3390/cells10113155.
25. Hurwitz SN, Rider MA, Bundy JL, Liu X, Singh RK, Meckes DG. Proteomic profiling of NCI-60 extracellular vesicles uncovers common protein cargo and cancer type-specific biomarkers. Oncotarget. 2016;7(52):86999–87015. doi:10.18632/oncotarget.13569.
26. White MJV, Roife D, Gomer RH. Galectin-3 binding protein secreted by breast cancer cells inhibits monocyte-derived fibrocyte differentiation. J Immunol. 2015;195(4):1858–1867. doi:10.4049/jimmunol.1500365.
27. Capone E, Iacobelli S, Sala G. Role of galectin 3 binding protein in cancer progression: a potential novel therapeutic target. J Transl Med. 2021;19(1):405. doi:10.1186/s12967-021-03085-w.
28. Fusco O, Querzoli P, Nenci I, Natoli C, Brakebush C, Ullrich A, Iacobelli S. 90K (MAC-2 BP) gene expression in breast cancer and evidence for the production of 90K by peripheral-blood mononuclear cells. Int J Cancer. 1998;79:23–26. doi:10.1002/(sici)1097-0215(19980220)79:1<23.
29. Loimaranta V, Hepojoki J, Laaksoaho O, Pulliainen AT. Galectin-3-binding protein: a multitask glycoprotein with innate immunity functions in viral and bacterial infections. J Leukoc Biol. 2018;104(4):777–786. doi:10.1002/JLB.3VMR0118-036R.
30. Powell TJ, Schreck R, McCall M, Hui T, Rice A, App H, Azam M, Ullrich A, Shawver LK. A tumor-derived protein which provides T-cell costimulation through accessory cell activation. J Immunother Emphasis Tumor Immunol. 1995;17(4):209–221. doi:10.1097/00002371-199505000-00003.
31. Ullrich A, Sures I, D'Egidio M, Jallal B, Powell TJ, Herbst R, Dreps A, Azam M, Rubinstein M, Natoli C, et al. The secreted tumor-associated antigen 90K is a potent immune stimulator. J Biol Chem. 1994;269(28):18401–18407. doi:10.1016/S0021-9258(17)32322-0.
32. Iacobelli S, Scambia G, Natoli C, Panici PB, Baiocchi G, Perrone L, Mancuso S. Recombinant human leukocyte interferon-α 2b stimulates the synthesis and release of a 90k tumor-associated antigen in human breast cancer cells. Int J Cancer. 1988;42(2):182–184. doi:10.1002/ijc.2910420207.
33. Gallo V, Arienzo A, Iacobelli S, Iacobelli V, Antonini G. Gal-3BP in viral infections: an Emerging role in severe acute respiratory syndrome coronavirus 2. Int J Mol Sci. 2022 Jun 30;23(13):7314. doi:10.3390/ijms23137314.
34. Yang L, Li J, Li S, Dang W, Xin S, Long S, Zhang W, Cao P. Lu J. Extracellular vesicles regulated by viruses and antiviral strategies. Front Cell Dev Biol. 2021;9:9. doi:10.3389/fcell.2021.722020.
35. Guo Y, Shen R, Yu L, Zheng X, Cui R, Song Y, Wang D. Roles of galectin-3 in the tumor microenvironment and tumor metabolism (Review). Oncol Rep. 2020;44:1799–1809. doi:10.3892/or.2020.7777.
36. Sawant DV, Yano H, Chikina M, Zhang Q, Liao M, Liu C, Callahan DJ, Sun Z, Sun T, Tabib T, et al. Adaptive plasticity of IL-10^{+} and IL-35^{+} T_{reg} cells cooperatively promotes tumor T cell exhaustion. Nat Immunol. 2019;20(6):724–735. doi:10.1038/s41590-019-0346-9.
37. Lawlor N, Nehar-Belaid D, Grassmann JDS, Stoeckius M, Smibert P, Stitzel ML, Pascual V, Banchereau J, Williams A, Ucar D, et al. Single cell analysis of blood mononuclear cells stimulated through either LPS or anti-CD3 and anti-CD28. Front Immunol. 2021;12:636720. doi:10.3389/fimmu.2021.636720.
38. Mohammed NBB, Antonopoulos A, Dell A, Haslam SM, Dimitroff CJ. Chapter six - the pleiotropic role of galectin-3 in melanoma progression: unraveling the enigma. In: Abbott KL Dimitroff CJ, editors. Advances in cancer research. Vol. 157. Academic Press; 2023. pp. 157–193. doi:10.1016/bs.acr.2022.06.001.
39. Foulds GA, Vadakekolathu J, Abdel-Fatah TMA, Nagarajan D, Reeder S, Johnson C, Hood S, Moseley PM, Chan SYT, Pockley AG, et al. Immune-phenotyping and transcriptomic profiling of peripheral blood mononuclear cells from patients with breast cancer: identification of a 3 gene signature which predicts relapse of triple negative breast cancer. Front Immunol. 2018;9:2028. doi:10.3389/fimmu.2018.02028.